

## Methods

### Whole-mount *in situ* hybridization

The ISH protocol was adapted from ref. 25 with the following modifications: embryos were fixed overnight in 4% paraformaldehyde in 0.1 M MOPS pH 7.5, 0.5 M NaCl at 4°C, washed in 0.05 M Tris-HCl pH 8, treated for 1 min with 10 µg ml<sup>-1</sup> proteinase K in 0.05 M Tris-HCl pH 8 at 37°C, followed by incubation in 1 M MOPS, 0.5 M NaCl, 0.1% Triton X-100 at 20°C for 20 min. Embryos were prehybridized for 1 h and hybridized overnight in 50% deionized formamide, 5 × SSC, 1% blocking reagent at 60°C. After the washing procedure, the hybridized embryos were blocked in 1% blocking reagent (Roche) and 1% filtered (0.45 µm pore size) lamb sera (Gibco) in PBS for 1 h at 20°C. They were then incubated for a further 1 h at 20°C in alkaline-phosphatase-coupled anti-digoxigenin Fab fragments (Roche) and in 1 × PBS, 0.1% Triton X-100 and treated for standard detection as described by Roche. Alternatively, the embryos were incubated in horseradish-peroxidase-conjugated anti-digoxigenin Fab fragments (Roche) for 4 h at 20°C, followed by 1–4 days of incubation at 20°C with the Tyramide Signal Amplification kit (Perkin Elmer) for fluorescence staining. Nuclear staining was obtained by incubation overnight at 4°C with To-Pro-3 iodide (Molecular Probes). Specimens were mounted in Vectashield mounting medium (Vector Laboratories) and analysed with a Leica TCS laser scanning confocal microscope.

Received 13 March; accepted 3 June 2004; doi:10.1038/nature02709.

1. Wada, H. Evolutionary history of free-swimming and sessile lifestyles in urochordates as deduced from 18S rDNA molecular phylogeny. *Mol. Biol. Evol.* **15**, 1189–1194 (1998).
2. Finnerty, J. R. The origins of axial patterning in the metazoan: how old is bilateral symmetry? *Int. J. Dev. Biol.* **47**, 523–529 (2003).
3. Balavoine, G., de Rossi, R. & Adoutte, A. *Hox* clusters and bilaterian phylogeny. *Mol. Phylogen. Evol.* **24**, 366–373 (2002).
4. Von Allmen, G. *et al.* Splits in fruitfly *Hox* gene complexes. *Nature* **380**, 116 (1996).
5. Burglin, T. R. & Ruvkun, G. The *Caenorhabditis elegans* homeobox gene cluster. *Curr. Opin. Genet. Dev.* **3**, 615–620 (1993).
6. Akam, M. *Hox* and *HOM*: homologous gene clusters in insects and vertebrates. *Cell* **57**, 347–349 (1989).
7. Ferrier, D. E., Minguillon, C., Holland, P. W. & Garcia-Fernandez, J. The amphioxus *Hox* cluster: deuterostome posterior flexibility and *Hox14*. *Evol. Dev.* **2**, 284–293 (2000).
8. Powers, T. P. & Amemiya, C. T. Evidence for a *Hox14* paralog group in vertebrates. *Curr. Biol.* **14**, R183–R184 (2004).
9. Dehal, P. *et al.* The draft genome of *Ciona intestinalis*: insights into chordate and vertebrate origins. *Science* **298**, 2157–2167 (2002).
10. Spagnuolo, A. *et al.* Unusual number and genomic organization of *Hox* genes in the tunicate *Ciona intestinalis*. *Gene* **309**, 71–79 (2003).
11. Seo, H. C. *et al.* Miniature genome in the marine chordate *Oikopleura dioica*. *Science* **294**, 2506 (2001).
12. Boutanaev, A. M., Kalmykova, A. I., Shevlyov, Y. Y. & Nurminsky, D. I. Large clusters of co-expressed genes in the *Drosophila* genome. *Nature* **420**, 666–669 (2002).
13. Roy, P. J., Stuart, J. M., Lund, J. & Kim, S. K. Chromosomal clustering of muscle-expressed genes in *Caenorhabditis elegans*. *Nature* **418**, 975–979 (2002).
14. Gionti, M. *et al.* *Cihox5*, a new *Ciona intestinalis* *Hox*-related gene, is involved in regionalization of the spinal cord. *Dev. Genes Evol.* **207**, 515–523 (1998).
15. Locascio, A. *et al.* Patternning the ascidian nervous system: structure, expression and transgenic analysis of the *Cihox3* gene. *Development* **126**, 4737–4748 (1999).
16. Nagatomo, K. & Fujiwara, S. Expression of *Raldh2*, *Cyp26* and *Hox-1* in normal and retinoic acid-treated *Ciona intestinalis* embryos. *Gene Expr. Patterns* **3**, 273–277 (2003).
17. Welsch, U. & Storch, V. Zur Feinstruktur der Chorda dorsalis niedriger Chordaten *Dendrodoa grossularia* (v. Beneden) und *Oikopleura dioica* (Fol.). *Z. Zellforsch. Mikrosk. Anat.* **93**, 547–559 (1969).
18. Lacalli, T. C. Tunicate tails, stolons, and the origin of the vertebrate trunk. *Biol. Rev. Camb. Phil. Soc.* **74**, 177–198 (1999).
19. Ferrier, D. E. & Holland, P. W. *Ciona intestinalis* *ParaHox* genes: evolution of *Hox*/*ParaHox* cluster integrity, developmental mode, and temporal colinearity. *Mol. Phylogen. Evol.* **24**, 412–417 (2002).
20. van der Hoeven, F., Zakany, J. & Duboule, D. Gene transpositions in the *HoxD* complex reveal a hierarchy of regulatory controls. *Cell* **85**, 1025–1035 (1996).
21. Averof, M. & Akam, M. *Hox* genes and the diversification of insect and crustacean body plans. *Nature* **376**, 420–423 (1995).
22. Kmita, M. & Duboule, D. Organizing axes in time and space: 25 years of colinear tinkering. *Science* **301**, 331–333 (2003).
23. Cowing, D. & Kenyon, C. Correct *Hox* gene expression established independently of position in *Caenorhabditis elegans*. *Nature* **382**, 353–356 (1996).
24. Aboobaker, A. A. & Blaxter, M. L. *Hox* gene loss during dynamic evolution of the nematode cluster. *Curr. Biol.* **13**, 37–40 (2003).
25. Spada, E. *et al.* Molecular patterning of the oikopleurid epithelium of the larvacean tunicate *Oikopleura dioica*. *J. Biol. Chem.* **276**, 20624–20632 (2001).
26. Swofford, D. L. *PAUP\* 4.0: Phylogenetic Analysis Using Parsimony (\*and other methods)*, Version 4.0b10 (Sinauer, Sunderland, Massachusetts, 2002).
27. Schmidt, H., Strimmer, K., Vingron, M. & von Haeseler, A. TREE-PUZZLE: maximum likelihood phylogenetic analysis using quartets and parallel computing. *Bioinformatics* **18**, 502–504 (2002).
28. Bassham, S. & Postlethwait, J. Brachury (T) expression in embryos of a larvacean urochordate, *Oikopleura dioica*, and the ancestral role of *T*. *Dev. Biol.* **220**, 322–332 (2000).

**Supplementary Information** accompanies the paper on [www.nature.com/nature](http://www.nature.com/nature).

**Acknowledgements** We thank A. Adoutte for advice throughout the course of this work; R. Asland, M. Schartl, T. Stach and E. Thompson for their comments at several stages of manuscript preparation; and the personnel of the *Oikopleura* culture facility for technical support. Funding was provided by the Research Council of Norway and the University of Bergen in the frame of the Sars Centre – EMBL partnership contract.

**Competing interests statement** The authors declare that they have no competing financial interests.

**Correspondence** and requests for materials should be addressed to D.C. (Daniel.Chourrout@sars.uib.no). BAC clone sequences have been deposited in GenBank under accession numbers AY449458–AY449462 and AY613855–AY613856.

## Biological abnormality of impaired reading is constrained by culture

Wai Ting Siok<sup>1</sup>, Charles A. Perfetti<sup>2</sup>, Zhen Jin<sup>3</sup> & Li Hai Tan<sup>1,4</sup>

<sup>1</sup>Cognitive Neuroscience Laboratory, Department of Linguistics, University of Hong Kong, Hong Kong, China

<sup>2</sup>Learning Research and Development Center, University of Pittsburgh, Pittsburgh, Pennsylvania 15260, USA

<sup>3</sup>MRI Division, Beijing 306 Hospital, Beijing 100101, China

<sup>4</sup>Laboratory of Neuropsychology, National Institute of Mental Health, NIH, Bethesda, Maryland 20892, USA

Developmental dyslexia is characterized by a severe reading problem in people who have normal intelligence and schooling<sup>1–3</sup>. Impaired reading of alphabetic scripts is associated with dysfunction of left temporoparietal brain regions<sup>2–5</sup>. These regions perform phonemic analysis and conversion of written symbols to phonological units of speech (grapheme-to-phoneme conversion); two central cognitive processes that mediate reading acquisition<sup>6–7</sup>. Furthermore, it has been assumed that, in contrast to cultural diversities, dyslexia in different languages has a universal biological origin<sup>1,8</sup>. Here we show using functional magnetic resonance imaging with reading-impaired Chinese children and associated controls, that functional disruption of the left middle frontal gyrus is associated with impaired reading of the Chinese language (a logographic rather than alphabetic writing system). Reading impairment in Chinese is manifested by two deficits: one relating to the conversion of graphic form (orthography) to syllable, and the other concerning orthography-to-semantics mapping. Both of these processes are critically mediated by the left middle frontal gyrus, which functions as a centre for fluent Chinese reading<sup>9–11</sup> that coordinates and integrates various information about written characters in verbal and spatial working memory. This finding provides an insight into the fundamental pathophysiology of dyslexia by suggesting that rather than having a universal origin, the biological abnormality of impaired reading is dependent on culture.

Unlike alphabetic writing systems that follow a design principle of mapping graphemes (visual form) onto phonemes (minimal phonological units of speech), the Chinese logographic system maps graphic forms (characters) onto morphemes (meanings). The phonology of written Chinese is defined at the monosyllabic level, with no parts of a character corresponding to phonemes. For instance, in the English word ‘beech’ the ‘b’ corresponds to /b/, and the latter is a segment of the word. However, the Chinese character 理 is pronounced /li3/ (meaning ‘reason’, where the numeral refers to Chinese tone), and its phonetic component 里, located on the right (also pronounced /li3/, meaning ‘inside’), does not correspond to a piece of the word’s phonological form. Hence, Chinese writing does not allow the segmental analysis that is fundamental to

alphabetic systems<sup>12</sup>, so the letter–sound conversion rules that exist for all alphabetic languages are impossible in Chinese. Visually, Chinese characters possess a number of intricate strokes that are packed into a square shape, often having their meanings suggested by visual configurations<sup>13</sup>.

The characteristics of written Chinese as a morphosyllabic system present a sharp contrast with the alphabetic system that provides the critical dimensions of universal comparisons. Whereas behavioural research has established that impaired reading of the English language is caused by phonological deficits (that is, a failure to form quality links between orthography and phonology), the characterization of reading impairments in Chinese might be different. Research has shown that reading in Chinese entails recurrent and parallel activations of three interconnected linguistic constituents: orthography, meaning and phonology<sup>14,15</sup>. On this view, reading difficulty in Chinese evolves not only from a poor quality mapping of orthography to phonology, but also from a substandard connection between orthography and semantics. Therefore, cortical activation irregularity associated with impaired Chinese reading is thought to differ from that associated with impaired English reading.

We performed two functional magnetic resonance imaging (fMRI) experiments to test this hypothesis. Experiment 1 sought to identify brain regions showing greater activation in normal Chinese readers during orthography-to-phonology mapping than in impaired Chinese readers. We used a homophone judgement design in which 16 children (average age 11) judged whether two synchronously exposed Chinese characters had an identical pronunciation (Fig. 1a; see Methods). In the control condition, children decided whether a pair of characters had the same physical size (font size decision). This task controlled for activation owing to the visual-orthographic and incidental semantic processing of the linguistic stimuli in the experimental task, thus allowing us to identify neural correlates of phonological processing and orthography-to-phonology mapping<sup>10,16</sup>. Analysis of variance revealed that normal readers performed better than impaired readers in homophone judgements (response accuracy,  $F_{1,13} = 4.744, P < 0.05$ , and reaction time,  $F_{1,13} = 8.258, P < 0.05$ ; Fig. 1d, e), but accuracy and

reaction time differences between homophone and font size decisions were not significant across normal and impaired readers ( $F$ -values  $< 1$ ). This indicates that our neuroimaging results from comparisons of task and control conditions in the two groups were not due to performance differences<sup>6</sup> or task difficulty<sup>17</sup>.

During homophone judgement (contrasted with font size decision), normal readers activated neural circuits involving left mid-inferior frontal gyrus, cingulate cortex and several regions in the occipital lobe (Table 1 and Fig. 2a), with 100% intersubject consistency particularly in mid-inferior frontal cortex and cingulate cortex (Fig. 2b). Impaired readers activated neural networks that essentially overlap those activated by normal readers, showing 100% intersubject consistency in left inferior prefrontal gyrus. Notably, direct comparisons of blood-oxygen-level-dependent (BOLD) activity of the two groups indicated that cortical activity was stronger in left middle frontal gyrus (LMFG) at Brodmann area (BA) 9 ( $x = -50, y = 11, z = 34$ ) for normal readers than for impaired readers (Fig. 2c). Conversely, in left inferior prefrontal gyrus (BA 45:  $x = -53, y = 23, z = 16$ ), impaired readers had stronger brain activation than normal readers (Fig. 2d). A correlation analysis of BOLD activation and children's reading performance indicated a significant positive correlation in LMFG ( $r = 0.529, P < 0.05$ ) and a significant negative correlation in left inferior frontal gyrus ( $r = -0.749, P < 0.001$ ), lending support to the results from group comparisons. Impaired readers showed activity in the left inferior parietal cortex, whereas normal readers

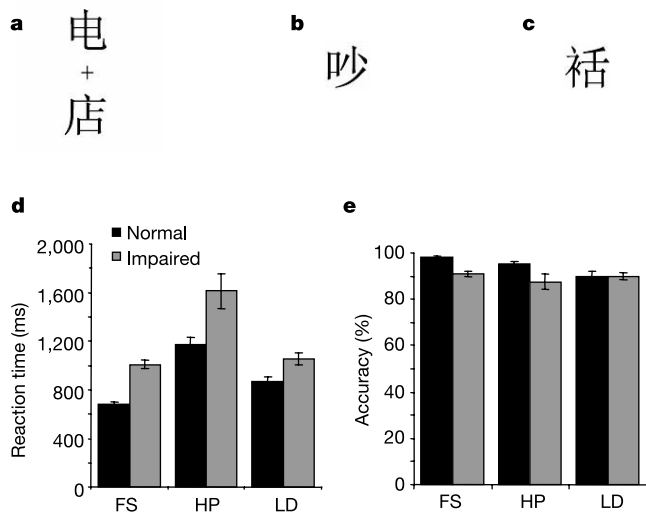


**Figure 1** Examples of experimental materials and behavioural results. **a**, Two homophonic characters (pronounced /dian/). **b**, A real Chinese character. **c**, A non-character. From these examples, it can be seen that Chinese characters are composed of a number of strokes and are salient as holistic square-shaped units. **d**, Reaction time. **e**, Accuracy. Error bars indicate standard error measurement (s.e.m.). FS, font size judgement; HP, homophone decision; LD, lexical decision.

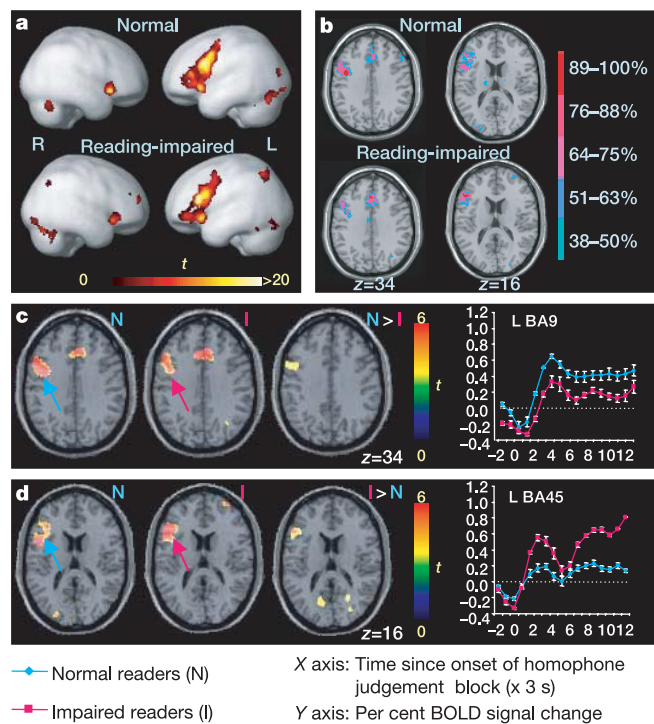


**Figure 2** Brain regions with significant activity during phonological processing and orthography-to-phonology mapping. **a**, Cortical activation associated with homophone judgement contrasted with font size decision in normal and reading-impaired Chinese readers. **b**, Intersubject consistency. LMFG activity was found in all normal readers, whereas left inferior prefrontal activity was found in all impaired readers. **c**, **d**, Brain regions showing group differences during homophone judgement. Presented are time course and activation maps in LMFG (**c**) and left inferior frontal gyrus (**d**) as indicated by blue (normal readers) and red (impaired readers) arrows. Per cent BOLD signal change ( $\pm$ s.e.m.) at voxels of maximal difference between groups is shown from the interval of  $-6$ – $36$  s. N  $>$  I, normal readers minus impaired readers; I  $>$  N, impaired readers minus normal readers.

Table 1 Coordinates of activation peaks

Brain area	Homophone judgement						Lexical decision				
	BA	Coordinates			t-score	BA	Coordinates			t-score	
		X	Y	Z			X	Y	Z		
<b>Normal readers</b>											
Frontal lobe											
L middle frontal gyrus	9	-42	14	33	11.45	9	-51	10	38	14.11	
	6	-46	0	48	8.38						
L inferior frontal gyrus	44	-48	11	23	11.96	44	-44	3	29	24.19	
L insula						-	-32	25	1	13.84	
R middle frontal gyrus						9	53	27	28	13.91	
						6	40	-3	50	8.97	
R inferior frontal gyrus	47	38	17	-8	8.14	44	46	9	25	20.73	
						47	34	21	-4	15.79	
Anterior cingulate gyrus	32	8	27	30	6.83	32	2	20	37	16.95	
Medial frontal gyrus	8	-2	18	47	12.21	8	-2	30	41	19.10	
Occipital lobe											
L fusiform gyrus	19	-34	-73	-13	6.39	19/37	-46	-65	-10	27.41	
	37	-34	-55	-12	5.47	37	-38	-53	-18	18.65	
L mid-inferior occipital	18	-26	-91	0	6.09	18	-28	-89	-1	19.34	
	19	-26	-85	19	5.81						
L lingual gyrus	18	-28	-76	-8	6.29						
Parietal lobe											
R inferior parietal lobule						40	48	-29	46	7.33	
Subcortical regions											
L thalamus						-	-10	-19	6	10.79	
R thalamus						-	6	-19	6	9.71	
						-	4	-10	4	9.18	
L cerebellum	-	32	-63	-22	6.91	-	-32	-74	-38	6.21	
<b>Reading-impaired readers</b>											
Frontal lobe											
L middle frontal gyrus	9	-38	6	38	7.35	9	-42	11	30	12.35	
						10	-30	40	18	7.56	
						46	-51	26	24	5.50	
L inferior frontal gyrus	45	-51	26	13	12.07	47	-32	19	-1	13.29	
	44/45	-42	13	21	11.75						
	47	-30	25	-5	11.73						
L precentral gyrus						4	-36	-21	54	8.73	
						4	-50	-19	49	8.58	
						4	-34	-28	62	5.15	
R superior frontal gyrus	10	32	57	14	5.98	6	-32	-2	31	6.70	
R middle frontal gyrus	10	22	44	20	5.70	10	38	53	7	11.11	
						46	44	25	21	9.99	
						6	34	2	50	8.24	
R inferior frontal gyrus	47	32	25	-6	10.28	47	36	21	-8	15.20	
	45	34	22	8	5.65						
Anterior cingulate gyrus	32	-2	19	40	13.04	32	4	23	34	17.42	
	32	10	26	21	6.59						
Medial frontal gyrus	8	-2	18	47	12.60	6	-4	-9	48	6.86	
Occipital lobe											
L superior occipital gyrus						19	-24	-70	31	9.53	
L fusiform gyrus	37	-38	-51	-18	6.16	37/18	-40	-76	-11	17.12	
L lingual gyrus	18	-6	-80	-14	6.40	18	-24	-93	0	18.65	
L middle occipital gyrus	19	-40	-72	-8	5.65	19	-38	-72	-3	16.80	
L cuneus	17	-16	-65	12	5.68						
	18	-12	-73	15	4.87						
R superior occipital gyrus	19	34	-62	40	5.84	37	40	-55	-17	17.64	
R fusiform gyrus						18	38	-80	1	16.59	
R mid-inferior occipital	18	32	-88	-6	6.30	19	36	-79	8	15.67	
R lingual gyrus	19	30	-56	1	5.45						
Parietal lobe											
L inferior parietal lobe	40/19	-30	-62	40	6.51	40/7	-26	-58	42	11.77	
L superior parietal lobe	7	-28	-64	47	6.50	7	-34	-52	56	8.66	
R inferior parietal lobe						40	48	-31	42	6.52	
Subcortical regions											
L thalamus	-	-12	-15	8	6.17	-	-28	-31	-3	8.28	
R thalamus						-	6	-17	12	8.77	
L cerebellum	-	-8	-85	-23	6.20						
	-	-30	-61	-17	5.55						
R cerebellum	-	8	-77	-21	8.45						
<b>Normal &gt; impaired readers</b>											
Frontal lobe											
L middle frontal gyrus	9	-50	11	34	4.16	9	-50	10	38	18.02	
L inferior frontal gyrus						44	-44	3	29	15.03	
R middle frontal gyrus						9	50	29	30	4.23	
R inferior frontal gyrus						44	44	5	26	11.69	
Occipital lobe											
L fusiform gyrus						19/37	-46	-65	-12	11.64	
<b>Impaired &gt; normal readers</b>											
Frontal lobe											
L inferior frontal gyrus	45	-53	23	16	12.07						
Occipital lobe											
R inferior occipital cortex						18	26	-78	-3	8.15	

L, left; R, right; normal &gt; impaired readers, normal readers minus impaired readers; impaired &gt; normal readers, impaired readers minus normal readers.

did not (Fig. 2a). However, the between-group comparison did not reveal this difference to be statistically significant, owing to low intersubject consistency (25%) of the activation of this brain area in impaired readers.

These results suggest that there is an important neurological difference with respect to impaired Chinese and English reading. Previous research using similar designs has consistently revealed reduced activation in left temporoparietal regions as a biological signature of English reading disability<sup>2,4,5</sup>. Furthermore, it has been shown that behavioural remediation ameliorates these dysfunctional neural mechanisms in American children with dyslexia<sup>3,5</sup>. In experiment 1, we observed reduced activation of LMFG, instead of left temporoparietal regions, as a neuro-anatomical marker of Chinese reading difficulty. Our findings agree with previous imaging data showing that LMFG is a crucial brain area responsible for skilled Chinese reading<sup>9–11</sup>. Broadly speaking, the LMFG carries out the representation and working memory of visuo-spatial and verbal information, and coordinates cognitive resources as a central executive system<sup>18–20</sup>. Chinese characters are composed of intricate strokes packed into a square shape; recognizing the character demands detailed visuo-spatial computation and, during homophone judgement, a high interactivity of orthography and phonology. The LMFG is recruited to serve these functions.

We also noted the hyperactivity of the anterior portion of the left

inferior prefrontal cortex (BA 45) arising during impaired Chinese reading. This finding is compatible with findings of English reading impairment<sup>4</sup>, suggesting that impaired Chinese reading engages neural circuits in anterior regions to compensate for the disruption in mid-dorsal frontal systems.

To determine whether brain regions mediating orthography-to-semantics mapping show abnormal activity in impaired Chinese reading, we performed a second experiment using the same subjects in a character decision design that required children to judge whether a viewed stimulus was a real Chinese character (Fig. 1b, c). This task focuses on the processing of visual-orthographic and semantic constituents and their interconnections (see Methods), although phonological information of ‘legal’ characters may also be relevant. Behavioural results indicated that normal readers performed better than impaired readers in reaction time (Fig. 1d;  $F_{1,14} = 9.14$ ,  $P < 0.01$ ), but not in response accuracy (Fig. 1e;  $F_{1,14} = 0.004$ ,  $P = 0.949$ ). Brain activations related to character decision (contrasted with fixation baseline) were seen bilaterally in mid-inferior frontal lobes, inferior parietal cortex and occipital cortex (Fig. 3a and Table 1), with very high intersubject consistency particularly in middle and inferior frontal gyri and visual cortex (Fig. 3b). Nevertheless, important differences in the magnitude of cortical activity were observed between normal and reading-impaired children (Fig. 3c–h). Impaired readers showed weaker activation than normal readers in the following areas: bilateral

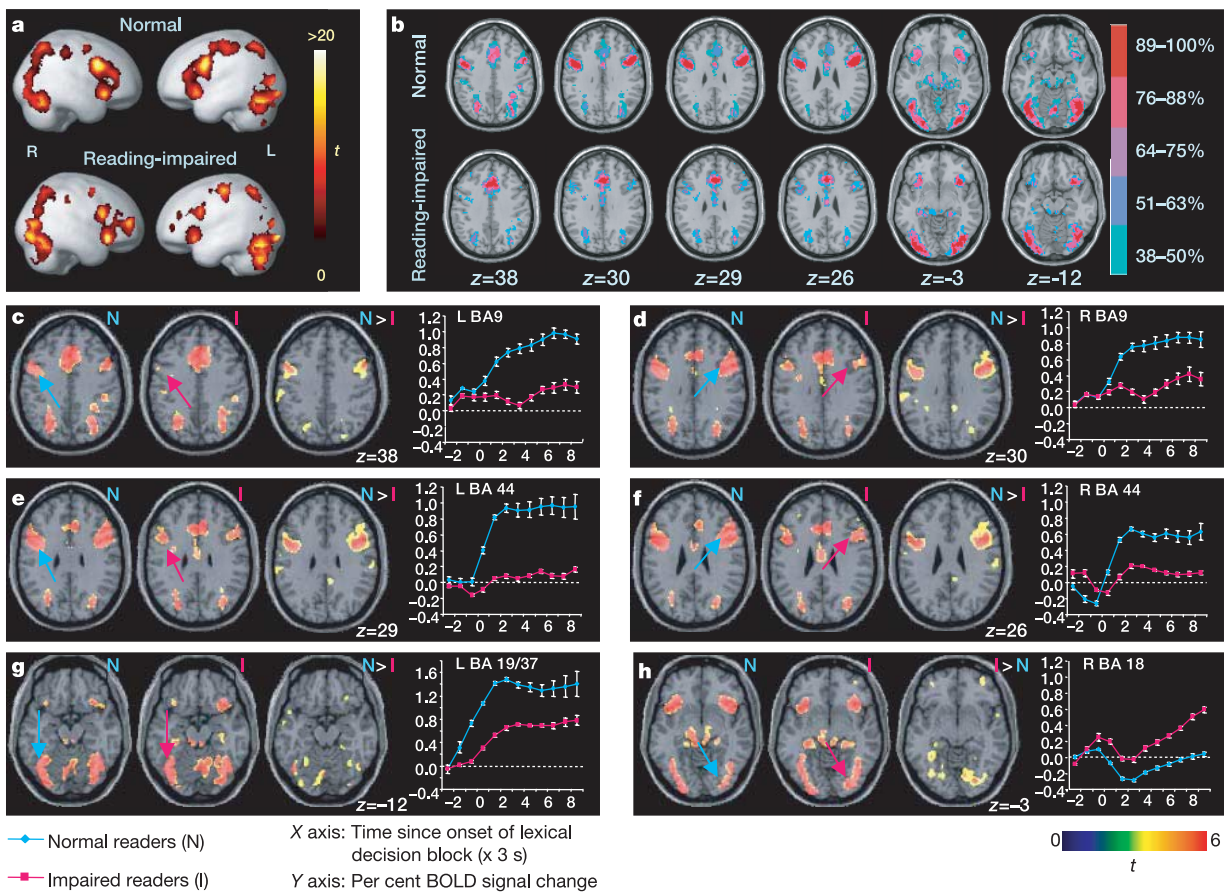


**Figure 3** Brain regions with significant activity during orthography-to-semantics mapping. **a**, Cortical activation associated with Chinese character decision (contrasted with fixation). **b**, Intersubject consistency. **c–h**, Group differences during character decision. Presented are time course and activation maps in LMFG, **c**; right MFG, **d**; left inferior frontal gyrus, **e**; right inferior frontal gyrus, **f**; left fusiform gyrus, **g**; and right BA 18, **h**.

inferior occipital cortex, **h**, as indicated by blue (normal readers) and red (impaired readers) arrows, respectively. Per cent BOLD signal change ( $\pm$ s.e.m.) at voxels of maximal difference between groups is shown from the interval of  $-6$ – $30$  s. N > I, normal readers minus impaired readers; I > N, impaired readers minus normal readers.

middle frontal gyrus at BA 9 ( $x = -50, y = 10, z = 38$  on the left, and  $x = 50, y = 29, z = 30$  on the right), bilateral inferior pre-frontal gyrus at BA 44 ( $x = -44, y = 3, z = 29$  on the left, and  $x = 44, y = 5, z = 26$  on the right), and left fusiform gyrus at BA 19/37 ( $x = -46, y = -65, z = -12$ ). Impaired readers showed greater activation than controls in right inferior occipital cortex near BA 18 ( $x = 26, y = -78, z = -3$ ). Correlation analyses of BOLD activation and reading performance revealed significant correlations in these brain regions (in left BA 9,  $r = 0.745, P < 0.001$ ; right BA 9,  $r = 0.707, P < 0.002$ ; left BA 44,  $r = 0.830, P < 0.001$ ; right BA 44,  $r = 0.814, P < 0.001$ ; left BA 19/37,  $r = 0.822, P < 0.001$ ; and right BA 18,  $r = -0.775, P < 0.001$ ).

Experiment 2 thus demonstrated a failure of large neural circuits to function properly during impaired Chinese reading. The reduced activation of LMFG agrees with the finding of experiment 1, suggesting that this brain region coordinates and integrates visual-orthographic and semantic (and phonological) processes in verbal and spatial working memory. This proposal is corroborated by our finding of greater activation in normal readers in left fusiform gyrus, a visual word form area that serves orthographic-to-semantic integration both in English<sup>21</sup> and Chinese<sup>22</sup>. The stronger activity of the posterior portion of the left inferior frontal gyrus for normal readers implies that this cortical region is particularly relevant to orthographic–semantic processing and also that controlled meaning retrieval<sup>23,24</sup> may mediate lexical decisions. The strong activity of left fusiform and inferiofrontal systems in normal Chinese reading seen in experiment 2 is in line with imaging studies of English reading development<sup>6</sup> and reading remediation<sup>3</sup>.

Two regions in the right hemisphere showed differences between normal and impaired Chinese readers. Normal readers showed stronger activation in right mid-inferior frontal gyrus, whereas impaired readers showed stronger activation in right inferior occipital cortex. Right mid-inferior frontal regions contribute to fluent Chinese reading<sup>9</sup>, and right inferior occipital cortex is thought to be engaged in visual processing of Chinese characters<sup>22,25</sup>. The increased activity of right inferior occipital gyrus in our experiment indicates that Chinese impaired readers struggle even in the visuo-spatial analysis of printed characters.

These two experiments provide compelling evidence that Chinese reading disability is characterized by the dysfunction of neural circuits responsible for the mapping of orthography-to-phonology and orthography-to-semantics. This pattern of findings is important for several reasons. First, it reveals a significant variation between the neural substrates of Chinese and English impaired reading. The LMFG is crucial to normal Chinese reading, as its dysfunction is associated with Chinese reading difficulty. Our findings support the idea that cognitive strategies for reading development tune the cortex<sup>26</sup>. This idea draws a parallel with a recent proposal that anatomical brain differences can be produced by differences in cultures, as suggested by a localized morphological analysis of brain anatomy that found that LMFG is anatomically larger in Chinese-speaking Asians than in English-speaking Caucasians<sup>27</sup>. Second, our fMRI findings showed that Chinese reading entails coherent and orchestrated activities of key neuroanatomical modules relating to orthography, semantics and phonology. This lends support to the assumption of parallel activation of meaning and phonology made by the interactive constituency model of (Chinese) reading<sup>14,15</sup>, while also posing a major challenge to the biological unity theory of dyslexia<sup>8</sup>. Finally, these data suggest that cross-cultural studies require great care to offer key dimensions of universal comparisons. Contrasts between writing systems with fundamental differences in their design principles, such as English and Chinese, allow understanding of both universal

and particular facets of the biological basis of reading disability. □

## Methods

Sixteen children underwent fMRI scans: eight impaired readers (six boys and two girls, mean age = 10 yr 11 months, range 10 yr 2 months to 12 yr 5 months) and eight normal reader controls (four boys and four girls, mean age = 11 yr 1 month, range 10 yr 5 months to 12 yr 4 months). The children were fourth and fifth graders from the Yuquan Primary School in Beijing, and were physically healthy and free of neurological disease, head injury and psychiatric disorder. All subjects participated in experiments 1 and 2. Because there is no standardized reading ability test in China, the classification of children's reading performance was based primarily on their school performance in the Chinese reading course and their teacher's recommendation. For impaired readers, reading scores in the school fell below the 5th percentile among all children in the same grade. Children defined as normal readers had reading scores above the 60th percentile. In addition, to assess reading ability and non-verbal IQ, a commonly used (but not standardized) reading test<sup>28</sup> comprising 120 Chinese characters and the Raven IQ test were administered to all 400 children in the fourth and fifth grades. The reading performance of these children was distributed normally, with an average score of 71 (s.d. = 14). The eight normal and eight reading-impaired subjects for our experiments had normal and matched non-verbal intelligence, with an average Raven IQ falling in the 92nd percentile for both groups. The reading-impaired group had a mean character reading score of 42, two standard deviations below the average and significantly discrepant from their normal, non-verbal intelligence. The two groups of children were significantly different in reading performance ( $t = 32.901, P < 0.001$ ). All children were native speakers of Putonghua, the official dialect of mainland China and the language of instruction in school. They were strongly right-handed as judged by the handedness inventory devised by Snyder and Harris<sup>29</sup>. Informed consent was obtained from each subject and their parents before testing.

## Design and materials

Experiment 1 used a phonological processing task; that is, homophone judgement. Experiment 2 used a character decision design (Fig. 1). The non-characters used in 'No' trials in experiment 2 were orthographically legal but without meanings or pronunciations (Fig. 1c). To perform the character decision successfully, children must rely on visual-orthographic familiarity and semantic accessibility of a viewed stimulus. All Chinese characters used in the two experiments were commonly encountered and selected from Chinese language textbooks of primary school grades 1 to 3. The visual complexity of the characters was matched across all conditions.

Each experiment was performed in a separate scan within the same session. In the homophone judgement scan, three blocks of homophone judgements were alternated with three blocks of font size judgements, which served as the baseline. Each block consisted of a 6-s instruction and 15 trials. In each trial, a pair of characters was synchronously exposed for 2,000 ms, one above and one below a fixation crosshair, followed by a 1,000-ms blank interval. In the character decision scan, four blocks of lexical decision task were alternated with four blocks of baseline task (visual fixation). Each task block consisted of a 6-s instruction and 20 trials. In each trial, a stimulus was displayed for 1,300 ms, followed by a 200-ms blank interval. For both experiments, subjects indicated a positive response by pressing the key corresponding to the index finger of their right (dominant) hand and a negative response by pressing the key corresponding to the index finger of their left (non-dominant) hand. They were asked to perform the tasks as quickly and accurately as possible. The behavioural data from one normal reader were not recorded correctly during the homophone judgement task and so were excluded from our statistical analysis of behavioural performance.

## MRI acquisition

MRI scans were performed on a 2 T GE/Elscint Prestige MRI scanner at Beijing 306 Hospital. Visual stimuli were presented to subjects through a projector onto a translucent screen. Subjects viewed the stimuli through a mirror attached to the head coil. A  $T_2^*$ -weighted gradient-echo echo planar imaging (EPI) sequence was used for fMRI scans, with the slice thickness = 6 mm, in-plane resolution =  $2.9 \times 2.9$  mm and repetition time/echo time/flip angle = 3,000 ms/45 ms/ 90°. Twenty contiguous axial slices were acquired parallel to the anterior commissure–posterior commissure (AC–PC) line covering the whole brain. High-resolution ( $2 \times 2 \times 2$  mm<sup>3</sup>) anatomical images were acquired using a  $T_1$ -weighted, three-dimensional gradient-echo sequence.

## Data analysis

SPM99 was used for image pre-processing and statistical analyses (<http://www.fil.ion.ucl.ac.uk/spm>). The functional images were realigned and normalized to an EPI template based on the ICBM152 stereotactic space (an approximation of canonical space). They were re-sampled into  $2 \times 2 \times 2$ -mm cubic voxels and spatially smoothed by an isotropic gaussian kernel (6 mm full width at half-maximum). Activation maps were generated by using the general linear model in which time series were modelled using a boxcar function for every condition and convolved with the canonical haemodynamic response function. Adjusted mean images were created for each condition after removing global signal and low-frequency covariates. For each group, contrast images between task and baseline conditions were computed using the  $t$  statistic, which generated statistical parametric maps of  $t$ -values. The voxelwise threshold was set at  $P < 0.05$  corrected for multiple comparisons, with an extent threshold of 20 contiguous voxels. Differences in activation maps between the two reading groups were examined with a two-sample  $t$ -test, and statistical threshold was set at  $P < 0.001$  uncorrected, with an extent threshold of

20 contiguous voxels. Brain regions were estimated from Talairach and Tournoux<sup>30</sup>, after adjustments for differences between MNI and Talairach coordinates. To evaluate the intersubject consistency of brain activations associated with normal and impaired reading in Chinese, we created penetrance maps by combining binary individual functional maps<sup>31</sup>. Penetrance maps were then overlaid on axial views of  $T_1$ -weighted images to demonstrate the voxels with significant activation in three or more subjects. The binary functional maps were determined using  $P < 0.05$  corrected for each subject.

Received 5 April; accepted 13 July 2004; doi:10.1038/nature02865.

1. Eden, G. & Moats, L. The role of neuroscience in the remediation of students with dyslexia. *Nature Neurosci.* **5**, 1080–1084 (2002).
2. Horwitz, B., Rumsey, J. M. & Donohue, B. C. Functional connectivity of the angular gyrus in normal reading and dyslexia. *Proc. Natl Acad. Sci. USA* **95**, 8939–8944 (1998).
3. Temple, E. *et al.* Neural deficits in children with dyslexia ameliorated by behavioral remediation: Evidence from functional MRI. *Proc. Natl Acad. Sci. USA* **100**, 2860–2865 (2003).
4. Shaywitz, S. E. *et al.* Functional disruption in the organization of the brain for reading in dyslexia. *Proc. Natl Acad. Sci. USA* **95**, 2636–2641 (1998).
5. Aylward, E. H. *et al.* Instructional treatment associated with changes in brain activation in children with dyslexia. *Neurology* **61**, 212–219 (2003).
6. Turkeltaub, P. E., Gareau, L., Flowers, D. L., Zeffiro, T. & Eden, G. Development of neural mechanisms for reading. *Nature Neurosci.* **6**, 767–773 (2003).
7. Rayner, K., Foorman, B. R., Perfetti, C. A., Pesetsky, D. & Seidenberg, M. S. How psychological science informs the teaching of reading. *Psychol. Sci. Publ. Interest* **2**, 31–74 (2001).
8. Paulesu, E. *et al.* Dyslexia: cultural diversity and biological unity. *Science* **291**, 2165–2167 (2001).
9. Tan, L. H. *et al.* The neural system underlying Chinese logograph reading. *Neuroimage* **13**, 836–846 (2001).
10. Tan, L. H. *et al.* Neural systems of second language reading are shaped by native language. *Hum. Brain Mapp.* **18**, 158–166 (2003).
11. Siok, W. T., Jin, Z., Fletcher, P. & Tan, L. H. Distinct brain regions associated with syllable and phoneme. *Hum. Brain Mapp.* **18**, 201–207 (2003).
12. Mattingly, I. G. in *Language by Ear and by Eye: The Relationships Between Speech and Reading* (eds Kavanagh, J. F. & Mattingly, I. G.) 133–147 (MIT Press, Cambridge, Massachusetts, 1972).
13. Wang, W. S.-Y. The Chinese language. *Sci. Am.* **228**, 50–62 (1973).
14. Perfetti, C. A. & Tan, L. H. in *Reading Chinese Script: A Cognitive Analysis* (eds Wang, J., Inhoff, A. W. & Chen, I.) 115–134 (Lawrence Erlbaum Associates, Mahwah, New Jersey, 1999).
15. Perfetti, C. A., Liu, Y. & Tan, L. H. The lexical constituency model: Some implications of research on Chinese for general theories of reading. *Psychol. Rev.* (in the press).
16. Price, C. J., More, C. J., Humphreys, G. W. & Wise, R. S. J. Segregating semantic from phonological processes during reading. *J. Cogn. Neurosci.* **9**, 727–733 (1997).
17. Gabrieli, J. D., Poldrack, R. A. & Desmond, J. E. The role of left prefrontal cortex in language and memory. *Proc. Natl Acad. Sci. USA* **95**, 906–913 (1998).
18. Courtney, S. M., Petit, L., Maisog, J. M., Ungerleider, L. G. & Haxby, J. V. An area specialized for spatial working memory in human frontal cortex. *Science* **279**, 1347–1351 (1998).
19. D'Esposito, M. *et al.* The neural basis of the central executive system of working memory. *Nature* **378**, 279–281 (1995).
20. Petrides, M., Alivisatos, B., Meyer, E. & Evans, A. C. Functional activation of the human frontal cortex during the performance of verbal working memory tasks. *Proc. Natl Acad. Sci. USA* **90**, 878–882 (1993).
21. Cohen, L. *et al.* The visual word form area: spatial and temporal characterization of an initial stage of reading in normal subjects and posterior split-brain patients. *Brain* **123**, 291–307 (2000).
22. Tan, L. H. *et al.* Brain activation in the processing of Chinese characters and words: A functional MRI study. *Hum. Brain Mapp.* **10**, 16–27 (2000).
23. Gold, B. T. & Buckner, R. L. Common prefrontal regions coactivate with dissociable posterior regions during controlled semantic and phonological tasks. *Neuron* **35**, 803–812 (2002).
24. Wagner, A. D., Pare-Blagoev, J. E., Clark, J. & Poldrack, R. A. Recovering meaning: left prefrontal cortex guides controlled semantic retrieval. *Neuron* **31**, 329–338 (2001).
25. Fu, S., Chen, Y., Smith, S., Iversen, S. & Matthews, P. M. Effects of word form on brain processing of written Chinese. *Neuroimage* **17**, 1538–1548 (2002).
26. Fiez, J. A. Sound and meaning: how native language affects reading strategies. *Nature Neurosci.* **3**, 3–5 (2000).
27. Kochunov, P. *et al.* Localized morphological brain differences between English speaking Caucasian and Chinese speaking Asian populations: New evidence of anatomical plasticity. *Neuroreport* **14**, 961–964 (2003).
28. Siok, W. T. & Fletcher, P. The role of phonological awareness and visual-orthographic skills in Chinese reading acquisition. *Dev. Psychol.* **36**, 887–899 (2001).
29. Snyder, P. J. & Harris, L. J. Handedness, sex, and familial sinistrality effects on spatial tasks. *Cortex* **29**, 115–134 (1993).
30. Talairach, J. & Tournoux, P. *Co-planar Stereotaxic Atlas of the Human Brain* (Thieme Medical Publishers, New York, 1988).
31. Fox, P. T. *et al.* A PET study of the neural system of stuttering. *Nature* **382**, 158–161 (1996).

**Acknowledgements** This work was supported by a Hong Kong Government RGC Central Allocation grant, and by the Intramural Research Program of NIMH. We thank J. Gabrieli, R. Desimone, C. K. Leong, K. K. Luke, S. Matthews and J. Spinks for support and comments.

**Competing interests statement** The authors declare that they have no competing financial interests.

**Correspondence** and requests for materials should be addressed to L.H.T. (lihaitan@intra.nimh.nih.gov).

## Reading the Hedgehog morphogen gradient by measuring the ratio of bound to unbound Patched protein

Andreu Casali & Gary Struhl

Howard Hughes Medical Institute, Department of Genetics and Development, Columbia University, New York, New York 10032, USA

Morphogens are ‘form-generating’ substances that spread from localized sites of production and specify distinct cellular outcomes at different concentrations. A cell’s perception of morphogen concentration is thought to be determined by the number of active receptors, with inactive receptors making little if any contribution<sup>1</sup>. Patched (Ptc)<sup>2–5</sup>, the receptor for the morphogen Hedgehog (Hh)<sup>6–12</sup>, is active in the absence of ligand and blocks the expression of target genes by inhibiting Smoothened (Smo), an essential transducer of the Hh signal<sup>13,14</sup>. Hh binding to Ptc abrogates the ability of Ptc to inhibit Smo, thereby unleashing Smo activity and inducing target gene expression<sup>2,3,12–16</sup>. Here, we show that a cell’s measure of ambient Hh concentration is not determined solely by the number of active (unliganded) Ptc molecules. Instead, we find that Hh-bound Ptc can titrate the inhibitory action of unbound Ptc. Furthermore, we demonstrate that this effect is sufficient to allow normal reading of the Hh gradient in the presence of a form of Ptc that cannot bind the ligand<sup>12</sup> but retains its ability to inhibit Smo. These results support a model in which the ratio of bound to unbound Ptc molecules determines the cellular response to Hh.

Hh signal transduction is unusual in that the unbound receptor (Ptc) is the active form (that is, it keeps the pathway switched ‘off’ by inhibiting the transducer (Smo)). Binding by the ligand (Hh) inactivates the receptor, releasing Smo from inhibition and turning the pathway on<sup>2,3,12–16</sup>. The cell’s perception of the amount of ambient Hh has been proposed to be determined solely by the number of unliganded (active) Ptc molecules<sup>17</sup>. Thus, as Hh rises from nil to peak concentrations, Smo activity would increase merely as a consequence of the progressive depletion of the pool of active Ptc protein. According to this depletion model, liganded Ptc would be functionally equivalent to the absence of Ptc. Alternatively, liganded Ptc might titrate the inhibitory activity of unliganded Ptc so that a cell’s perception of Hh concentration would depend on the ratio of the two forms<sup>12</sup>.

To distinguish these possibilities, we have expressed different levels of constitutively active Ptc<sup>Δloop2</sup> protein, a deleted form of Ptc (Fig. 1a) that cannot bind Hh but can still repress Smo<sup>12</sup>, and asked whether the minimum amount of Ptc<sup>Δloop2</sup> necessary to shut down the pathway depends on the presence of liganded Ptc. In the simple depletion model, in which Hh binding merely inactivates Ptc, Ptc<sup>Δloop2</sup> should be impervious to liganded Ptc, and the minimum amount of Ptc<sup>Δloop2</sup> required to turn off the pathway should not change. In the titration model, the presence of liganded Ptc should counteract the inhibitory activity of Ptc<sup>Δloop2</sup>, requiring higher levels of Ptc<sup>Δloop2</sup> to keep the pathway off.

Three Flp-out transgenes<sup>6</sup> called  $L > P^{\Delta 2}$ ,  $M > P^{\Delta 2}$  and  $H > P^{\Delta 2}$  (Fig. 1b; see Methods) were used to express low, medium or high levels of Ptc<sup>Δloop2</sup> protein in clones of imaginal wing disc cells (Fig. 1b; see Methods). Wing discs are subdivided into anterior and posterior compartments, with cells in the posterior compartment programmed to express and those in the anterior compartment to respond to Hh<sup>9,18</sup>. Ptc is normally expressed in anterior compartment cells only at low levels, except in those anterior cells that are located close to the anteroposterior compartment boundary